The 2009 IEEE/RSJ International Conference on
Intelligent Robots and Systems
October 11-15, 2009 St. Louis, USA

Development and Sensitivity Analysis of a Portable Calibration System for Joint Offset of Industrial Robot

Yong Liu, Ning Xi, Jianguo Zhao, Erick Nieves-Rivera, Yunyi Jia, Bingtuan Gao, Jun Lu

Abstract - **This paper describes our updated system for industrial robot joint offset calibration. The system consists of an IRB1600 industrial robot, a laser tool attached to the robot's end-effector, a portable position-sensitive device (PPD), and a PC based controller. By aiming the laser spot to the center of position-sensitive-detector (PSD) on the PPD with different robot configurations, the developed system ideally implements our proposed calibration method called the virtual line-based single-point constraint approach. However, unlike our previous approach, the calibration method is extended to identify the offset parameters with an uncalibrated laser tool. The position errors of the PPD and the sensitivities of error in the PSD plane to the variation of joint angles are analyzed. Two different robot configuration patterns are compared by implementing the calibration method. Both simulation and real experimental results are consistent with the mathematical analysis. Experimental results with small (10^{-3}-10^{-2}) mean and standard deviation of parameters error verify the effectiveness of both the sensitivity analysis and the developed system.**

Index Terms – **robot, joint offset calibration, sensitivity, development**

I. Introduction

It is well known that robot has high repeatability but low accuracy. Researchers have been working to improve the accuracy of industrial robots. With the industrial robot widely used in the complicated tasks requiring continuous path or precise localization, eg., arc welding, cutting, surgery, and anything else based on offline programming, etc., accuracy of the robot is more and more important.

Although there are many sources of inaccuracy, such as gear errors, thermal expansion, and structural deformations, the main source of the inaccuracy lies in the parameter errors of robot kinematics model. Robot calibration is an efficient way to improve the accuracy. There has been considerable research in this field. Robot kinematic parameters calibration methodologies and systems have been developed [1]-[5]. One kind of method relies on highly precise equipment measuring the robot end-effector pose, eg., coordinate measurement machines (CMM) [1] and laser tracking system [2]. However, the process is time/manpower consuming, and the device is expensive.

The other kind of method imposes some constraints on the end-effector to form closed kinematic chains [3] [4] [5]. These methods suffer from inexact positioning and time consuming. Newman et al. [6] and Chen et al. [7] proposed a calibration method using laser line tracking. Gatla et al. [8] described the virtual closed kinematic chain method. They gave the simulated results and did not implement a practical calibration system.

In addition, once the robot is shipped from the robot manufacture and installed for the user, some kinematic parameters, such as the link length, link twist and link offset, related to the mechanical structure of the robot itself, do not change too much, typically. However, some kinematics parameters such as joint offset might be changed more often because of the assembly or the replaced motors and encoders. What is more, the joint offset change only a little, then the positional accuracy is affected significantly. According to [6][7], more than 90% of the positional inaccuracy issues of the industrial robot are caused by the robot offset.

To fit this requirement of joint offset calibration, a new parameter calibration approach called virtual lines-based single-point constraint (VLBSPC) is proposed and a calibration device based on PSD and laser was implemented in our paper [9]. Unlike previous calibration methods, this approach does not need any physical contact and the developed device is affordable. The proposed method depends mainly on a laser pointer attached on the end-effector of a robot and only one PSD.

However, it is essential to develop a portable and affordable device for industrial robot joint offset calibration that can be used widely and frequently in the user factory, not only in the robot factory. That is to say, an offset calibration system that is fast, automated, and highly precise, most important, more low-cost and compact design will have high demand in manufacturing using industrial robots. In this paper, the newly developed calibration device is implemented and presented in detail. Based on the platform, the feedback errors of the PPD and the sensitivities of variations of joint values to the robot configuration and PSD position are analyzed.

In addition, parameters of the laser line are changed often because of the installation and laser spot adjustment. Hence,

This research work is partially supported by ABB University Research Program.

Yong Liu is with Department of Electrical and Computer Engineering Michigan State University East Lansing, MI 48824, USA, and Nanjing University of Science and Technology, Nanjing, China (e-mail: liuy1602@msu.edu)

Ning Xi is with the Department of Electrical and Computer Engineering, Michigan State University, East Lansing, MI 48824, USA, and also serving as an affiliate professor at the Shenyang Institute of Automation, Chinese Academy of Science, Shenyang, China (e-mail: xin@egr.msu.edu).

Jianguo Zhao, Erick Nieves-Rivera, Yunyi Jia, Bingtuan Gao and Jun Lu are with Department of Electrical and Computer Engineering, Michigan State University East Lansing, MI 48824, USA (e-mail: {zhaojia1, nieveser, jiayunyi, carlgao, lujun331}@msu.edu).

in this paper calibration parameters were extended to both joint offset and the laser line parameters at the same time. Calibration experiments referring to the configurations of the robot and PSD position are discussed. One is the location of the PSD changed, and the other is the different types of positions and orientations of end-effector loading the laser lines aiming towards the center of the PSD. Both simulation and real experiments implemented on an ABB industrial robot (IRB1600) verified the effectiveness of both the proposed method and the developed system.

This paper is structured as follows: the updated calibration system is presented in Section II. The modeling, mapping, errors, and sensitivities analysis of offset calibration are described in Section III. Both simulation and experimental results are demonstrated in Section IV. Finally, we conclude the work.

II. PORTABLE CALIBRATION SYSTEM

Fig. 1 shows the schematic design of robot offset calibration system, which is implemented and verified on an ABB robot as laboratory test-bed, shown in Fig. 2. The robot includes an ABB robot controller (IRC5) and a 6-DOF manipulator (IRB1600).

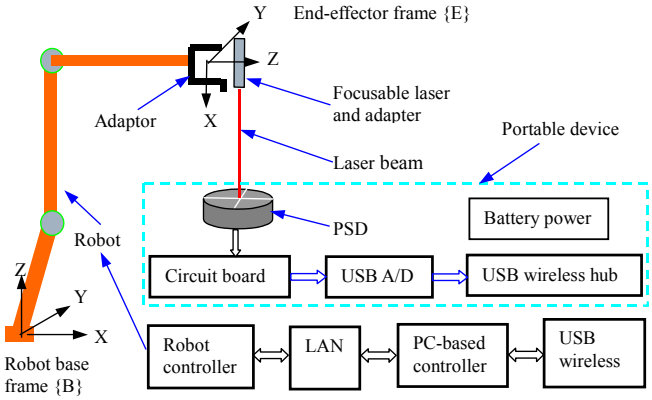

Fig.1. Schematic of the portable calibration system

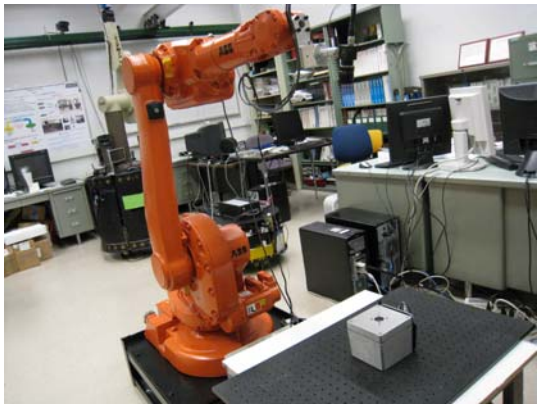

Fig.2. ABB robot and newly developed calibration system

The calibration system consists of battery-powered laser and laser adapter, as shown in Fig. 3(a), and portable position-sensitive device, as shown in Fig. 3(b). The portable position-sensitive device is equipped with battery, DC power, PSD interface tuning circuit, USB analog acquiring module and USB wireless device.

A single segmented PSD is employed and mounted on the fixture. The fixture is arbitrarily located on the robot workspace. The center point of the PSD is supposed to be the single-point constraint. The interface circuit is well designed and the signal tuning board can process the raw output of the laser spot on the PSD surface for two-dimension position feedback. USB-1408FS is used to acquire the analogy signal from the processing board.

PC-based controller performs collecting PSD output by wireless, PSD-based positioning servo and calibration algorithm. Through the network-based communication between robot controller and the PC-based controller, the latter can obtain the current robot position information (task space and joint space) from the robot controller and send the control command to the robot controller as well as update the target position in real-time.

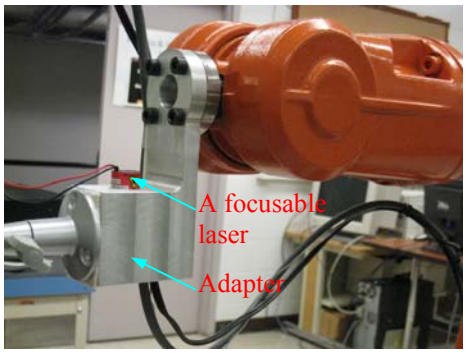

(a) The laser and adapter attached on the end-effector

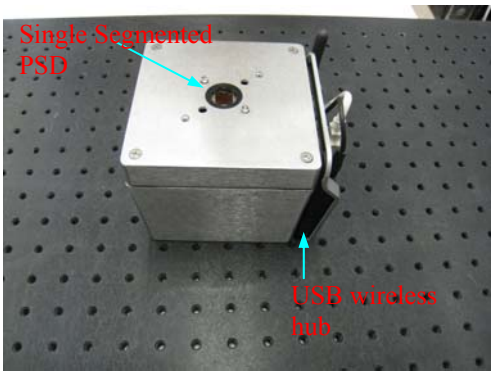

(b) The portable calibration device

Fig.3. Newly developed calibration device

III. CALIBRATION MODELING AND ANALYSIS OF ERRORS

A. Kinematic Error Model

The Denavit-Hartenberg [10] is a widely used convention for frame of reference in the forward kinematics. A model of the IRB1600 robot according to DH conventions is built [9]. Consider the joint offset, let δ_i denote the offset value of the ith joint, in the DH convention each homogeneous transformation is represented as,

$$\tilde{T}_i = \begin{bmatrix} c\tilde{\theta}_i & -s\tilde{\theta}_i c\alpha_i & s\tilde{\theta}_i s\alpha_i & a_i c\tilde{\theta}_i \\ s\tilde{\theta}_i & c\tilde{\theta}_i c\alpha_i & -c\tilde{\theta}_i s\alpha_i & a_i s\tilde{\theta}_i \\ 0 & s\alpha_i & c\alpha_i & d_i \\ 0 & 0 & 0 & 1 \end{bmatrix} \quad (3)$$

where use notation $c\tilde{\theta}_i$ for $cos(\theta_i + \delta_i)$ and $s\tilde{\theta}_i$ for $\sin(\theta_i + \delta_i)$.

Combining the joint offset and the six coordinate frames, forward kinematics ${}^bT_e$ with the offset error is written as,

$${}^bT_e = \tilde{T}_1\tilde{T}_2\tilde{T}_3\tilde{T}_4\tilde{T}_5\tilde{T}_6 \ . \quad (4)$$

B. Uncalibratied Laser Tool

A laser tool, a focusable laser pointer with its adapter, is rigidly attached on the end-effector of the robot. The laser line is adjusted to roughly align its orientation toward the x-axis in the end-effector frame. Let (M_E, N_E, P_E) denote the unit direction vector and (x_{0E}, y_{0E}, z_{0E}) denote the position of a point of the laser line in the end-effector frame. Once the laser pointer and the adapter is fixed, the laser line in the end-effector frame is given by

$$\frac{x_E - x_{0E}}{M_E} = \frac{y_E - y_{0E}}{N_E} = \frac{z_E - z_{0E}}{P_E} \ . \quad (5)$$

Note the values of (M_E, N_E, P_E) and (x_{0E}, y_{0E}, z_{0E}) are unknown. However, the number of independent parameters is 4 for the laser line (let $\kappa = \{M_E, N_E, y_{0E}, z_{0E}\}$). One of vector is dependent and x_{0E} is the offset along the x-axis in the end-effector frame (let x_{0E}=0). Joint 1 is dependent to the base frame and joint 6 is dependent to the parameter of laser line. Thus, the total number of calibration parameters to be identified is 8 (4 joint offsets + 4 laser line parameters).

C. Calibration Pattern and Calibration Method

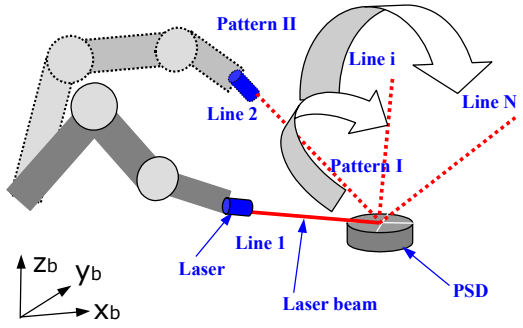

Robot base frame {B}

Fig.4. Schematic of calibration procedure

The calibration method represented in [9] relies mainly upon a laser pointer attached on the end-effector of a robot and single PSD. The calibration procedure is aiming a laser beam from the laser pointer at the same point from various positions and orientations by using hybrid visual/PSD servoing [11], as shown in Fig. 4. The same point is the center point of the PSD, and the coordinates of the point in the robot base frame are unknown. The calibration pattern of aiming the laser at the point from right side of the PSD to left side is called pattern I configuration. Correspondingly, that from the back to the front is called pattern II configuration. It is obvious that these patterns determine the robot configuration. The configuration effect on calibration solution will be discussed in the next section.

Suppose N sets of joint angle are recorded after PSD based localization. Combing the matrix equation (4) and equation (5), laser lines will be represented in the robot base fame. Let Γ_{Li} denote the *i*th laser line, P_k denote the intersection or the center of the shortest distance between Γ_{Li} and Γ_{Lj} ($i \neq j, i, j = 1, \cdots, N, k = 1, \cdots, M$), and ${}^nP_{Ave}$ denote the mean point of the total intersections P_k ($k = 1, \cdots, M$). The coordinate errors of the points between P_k and ${}^nP_{Ave}$ are denoted as ${}^x\Psi_k, {}^y\Psi_k, {}^z\Psi_k$ in the x, y, z directions, separately. The parameters $\Phi(\delta, \kappa)$ of joint offset and laser line are identified by minimizing the total sum of the squares of the coordinate errors.

$$\Phi(\delta,\kappa)^* = \arg\min_{\Phi(\delta,\kappa)} \sum_{k=1}^{M} \left({}^x\Psi_k{}^2 + {}^y\Psi_k{}^2 + {}^z\Psi_k{}^2 \right) \quad (6)$$

where M is the number of the intersections between laser lines. Note ${}^nP_{Ave}$ is updated during the minimization iteration process and P_k is the center of the line of the shortest distance from the lines between Γ_{Li} and Γ_{Lj} if the two lines do not have a real intersection.

The solution for the non-linear optimization is Levenberg-Marquardt algorithm (LMA) [12]. The optimum algorithm is a damped Gauss-Newton method based on the Jacobian J and damping parameter μ. The step h_{lm} is defined by

$$\left(J^T J + \mu I\right) h_{lm} = -g \quad (7)$$

where $g = J^T\Psi$, $\Psi = [\psi_1, \psi_2 \cdots \psi_k]^T, k = 1, \cdots, M$; $\psi_k = {}^x\psi_k{}^2 + {}^y\psi_k{}^2 + {}^z\psi_k{}^2$ and $\mu \geq 0$.

D. Measurement Sensitivities of the PPD

The active area of the PSD is 10mm in diameter and the laser spot shooting on the PSD surface is about 2.5mm in diameter. To map the PSD sensing device (both PSD and the conditioning circuit), a laser pointer was fixed on a computer aided probe (Signatone CAP 945) perpendicular to the PSD surface. The probe allows it to position the laser beam in 2 DOF (*x, y*) crossing the PSD surface with high precision (accuracy: ±2.5 μm, repeatability: ±1 μm, resolution: 40 *n*m per step).

The result of the whole active area sweeping along the y-axis is shown in figure 5(a) and that of the central area is shown in figure 5(b). From the figure 5(a) and 5(b), the

output voltage of the device is nonlinear to the position of laser spot on the PSD and the central area of the PSD has much better linearity and high sensitivity than other area.

At the case of robot calibration, the center of PSD is desired position of robot localization. From figure 5(b), the sensitivity is about 0.1 volt per 20μm within the central area (from –0.6mm to 0.6mm). Based on observation from experiments, the measurement noise is within ± 0.01 volt and consequently the error of the position is $\pm 2\mu m$ in the x-axis and y-axis, respectively.

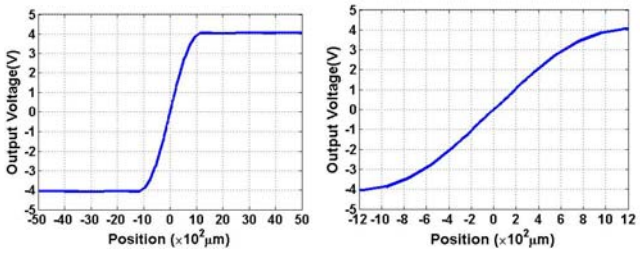

(a) (b)

Fig. 5. (a) Plot of the data of sweep along the y-axis in the whole active area. (b) Plot of the data of sweep along the y-axis in the central area.

E. Localization Sensitivities Analysis in Joint Space

The PSD has the high resolution with better than 0.1μm in theory, and actually the PPD has the resolution of approximately 2μm under this experimental condition. The accuracy of robot localization should be between $\pm 2\mu m$ and $\pm 50\mu m$ (repeated accuracy) based on PPD feedback. Thus it is important to know the sensitivities of the variations of the laser spot positions in the PSD plane to variations of joint angles at the robot joint space. Let Δ denote the sensitivities and ∂L denote variation of the laser spot in distance with the variation $\partial\Theta$ of joint angles. Then the sensitivities is given

$$\Delta = \partial L / \partial \Theta \ . \tag{8}$$

The position and orientation of the end-effector can be represented by $(P_x, P_y, P_z, \phi, \theta, \psi)$ with respect to the base frame. The laser is fixed on the end-effector and roughly parallel to the x-axis in the end-effector frame. The distance between the laser pointer and PSD surface is varying and approximately $\ell = 600$ mm. It is obvious the small variations in orientation of laser pointer in the end-effector are magnified on the PSD surface. Without loss of generality, assume the PSD is parallel to the X-Y plane in the base frame and robot locates in the initial position. The end-effector (joint 4) is rotated ζ about X-axis w.r.t the base frame. Hence, the variation of the laser spot on the PSD surface in the y-axis is

$$\Delta P_y = \ell \sin(\zeta) \tag{9}$$

Let the variations $\Delta P_y = 0.02$ mm, then

$$\zeta = 0.002 \text{ degree}$$

In this case, if the error from robot localization based on PSD servoing is less than 0.02mm, the error of joint 4 will be less than 0.002 degree. Fig. 6 shows the variations of the laser spot positions in the PSD plane to variations of joint 3. Other joint angles have the similar magnitude. However, note that the sensitivities vary with the robot configuration and actually it depends on the calibration system Jacobian. This is not discussed in the paper.

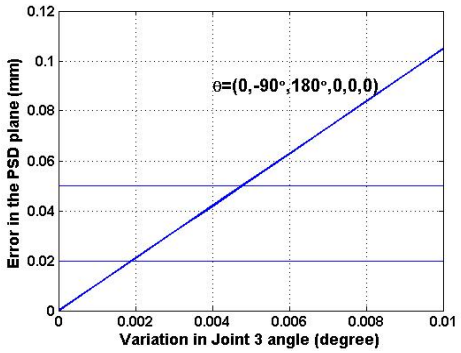

Fig.6. Changes in the PSD plane with variation of joint 3 angle.

F. Effect of Configuration on the Solution

Based on the PSD feedback, the laser beam precisely aimed on the center (unknown position) of the PSD at pattern I or pattern II. Then N sets of joint angles are recorded, and LMA is employed to identify the parameters. The convergent step h_{lm} is determined by (7) and is sensitive to the Jacobian J (note it is different from manipulator Jacobian). The position of PSD and the calibration pattern play an effect on the Jacobian. It can be proved mathematically by the relationship between the change in the intersection of two laser lines and the variation of joint angles. Without loss of generality, assume aiming a laser beam at the same point P_p from two positions P_A and P_B. Accordingly the joint angles are recorded as $(\theta_{11}, \theta_{21}, \theta_{31}, \theta_{41}, \theta_{51}, \theta_{61},)$ at P_A and $(\theta_{12}, \theta_{22}, \theta_{32}, \theta_{42}, \theta_{52}, \theta_{62},)$ at P_B, respectively. Let P_p coordinates in the base frame be

$$P_p = \begin{Bmatrix} p_x \\ p_y \\ p_z \end{Bmatrix}.$$

Substituting the joint angles into (4) and the point P_p with different orientation can be represented by

$$P_p{}^1(\theta_{11}, \theta_{21}, \theta_{31}, \theta_{41}, \theta_{51}, \theta_{61}) = \tilde{T}_1 \tilde{T}_2 \tilde{T}_3 \tilde{T}_4 \tilde{T}_5 \tilde{T}_6 \tilde{T}_7{}^1 \tag{10}$$

$$P_p{}^2(\theta_{12}, \theta_{22}, \theta_{32}, \theta_{42}, \theta_{52}, \theta_{62}) = \tilde{T}_1 \tilde{T}_2 \tilde{T}_3 \tilde{T}_4 \tilde{T}_5 \tilde{T}_6 \tilde{T}_7{}^2 \tag{11}$$

where $\tilde{T}_7$ denote the transformation matrix of the laser spot frame w.r.t the end-effector frame. Let ${}^2T_7$ denote the transformation matrix of the laser spot w.r.t the joint 2 frame. Then at the positions P_A and P_B, ${}^2T_7$ can be represented as

$${}^2T_7{}^1 = \begin{bmatrix} a_{11} & a_{12} & a_{13} & p_{1x} \\ a_{21} & a_{22} & a_{23} & p_{1y} \\ a_{31} & a_{32} & a_{33} & p_{1z} \\ 0 & 0 & 0 & 1 \end{bmatrix} \quad {}^2T_7{}^2 = \begin{bmatrix} b_{11} & b_{12} & b_{13} & p_{2x} \\ b_{21} & b_{22} & b_{23} & p_{2y} \\ b_{31} & b_{32} & b_{33} & p_{2z} \\ 0 & 0 & 0 & 1 \end{bmatrix}. \tag{12}$$

Consider the same point constraints at the two position, we have

$$p_x = p_{1x}c\theta_{11}s\theta_{21} + p_{1y}c\theta_{11}c\theta_{21} - p_{1z}s\theta_{11} + 0.7c\theta_{11}s\theta_{21} + 0.15c\theta_{11} \quad (13)$$
$$= p_{2x}c\theta_{12}s\theta_{22} + p_{2y}c\theta_{12}c\theta_{22} - p_{2z}s\theta_{12} + 0.7c\theta_{12}s\theta_{22} + 0.15c\theta_{12}$$

$$p_y = -p_{1x}s\theta_{11}c\theta_{21} + p_{1y}s\theta_{11}c\theta_{21} + p_{1z}c\theta_{11} + 0.7s\theta_{11}s\theta_{21} + 0.15s\theta_{11} \quad (14)$$
$$= -p_{2x}s\theta_{12}c\theta_{22} + p_{2y}s\theta_{12}c\theta_{22} + p_{2z}c\theta_{12} + 0.7s\theta_{12}s\theta_{22} + 0.15s\theta_{12}$$

$$p_z = p_{1x}c\theta_{21} - p_{1y}s\theta_{21} + 0.7c\theta_{21} + 0.15s\theta_{11} \quad (15)$$
$$= p_{2x}c\theta_{22} - p_{2y}s\theta_{22} + 0.7c\theta_{22} + 0.15s\theta_{12}$$

If the center of PSD locates on the x-axis in the base frame, then $p_y = 0$, and if pattern II (robot move from the front to the back) is used, then $\theta_{11} = \theta_{12} = 0$. Thus (13) and (15) can be given

$$p_x = p_{1x}s\theta_{21} + p_{1y}c\theta_{21} + 0.7s\theta_{21} = p_{2x}s\theta_{22} + p_{2y}c\theta_{22} + 0.7s\theta_{22}. \quad (16)$$

$$p_z = p_{1x}c\theta_{21} - p_{1y}s\theta_{21} + 0.7c\theta_{21} = p_{2x}c\theta_{22} - p_{2y}s\theta_{22} + 0.7c\theta_{22}. \quad (17)$$

If joint 2 has a same variation $\Delta\theta$, let $(16)\times c\Delta\theta + (17)\times s\Delta\theta$ and $(17)\times c\Delta\theta - (16)\times s\Delta\theta$, then we have

$$p_x' = p_{1x}s\theta_{21}' + p_{1y}c\theta_{21}' + 0.7s\theta_{21}' = p_{2x}s\theta_{22}' + p_{2y}c\theta_{22}' + 0.7s\theta_{22}'$$
$$p_z' = p_{1x}c\theta_{21}' - p_{1y}s\theta_{21}' + 0.7c\theta_{21}' = p_{2x}c\theta_{22}' - p_{2y}s\theta_{22}' + 0.7c\theta_{22}'$$

where $\theta' = \theta + \Delta\theta$. These results prove that in this case ${}^x\Psi_k, {}^y\Psi_k, {}^z\Psi_k$ are totally not related to the variation of joint 2 and thus joint 2 offset can not be identified.

Furthermore, if $p_y \to 0$ and pattern II is employed, then $\theta_{11} = \theta_{12} \to 0$. ${}^x\Psi_k, {}^y\Psi_k, {}^z\Psi_k$ are still not sensitive to the variation of joint 2. If there are some noises added to the joint angles, the real parameters are difficult to be identified because of local minimum. Even if p_y is not close to zero, the change of joint 1 angle is very small under the pattern II, then the joint 1 angle is close to a constant. Thus it still suffers from the similar result. However, it is free from the problem under pattern I because the joint 1 angle changes a lot.

IV. EXPERIMENTAL RESULTS AND DISCUSSION

A. Robot Localization

The real robot is limited to encoder resolution and noise. Experiments of robot localization were implemented on the IRB1600 industrial robot. Manipulator is roughly located within the active area of PSD surface with pre-designed pose by visual servo control. Thus controller is switched to PSD-based servo that precisely aims the laser line at the center of the PSD. At different unknown PSD position #1 and #2, the experiment of robot localization is repeated multiple times with seven different end-effector positions and orientations at pattern I and pattern II, respectively.

Table I shows the standard deviation of errors in joint space for robot localization at position #1 and position #2. From the table I, generally the standard deviation of errors was very small (from 10^{-2} to 10^{-3}), indicating that the robot localization based on PSD feedback is stable and precise. In addition, for pattern I, the standard deviation of errors at the position #2 is much smaller than that at the position #1. However, the errors are close at position #1 and #2 for pattern II. These results also show that the sensitivities of variation of joint values to localization errors rely on the robot configuration and the PSD positions.

TABLE I
THE RESULTS OF ROBOT LOCALIZATION IN JOINT SPACE

Joint	Pattern II STD ($\times 10^{-3}$)		Pattern I STD ($\times 10^{-3}$)	
	#1	#2	#1	#2
J1 (deg)	6.2	6.3	6.3	3.1
J2 (deg)	7.5	8.6	8.1	3.0
J3 (deg)	10	11.1	7.1	2.9
J4 (deg)	51.5	33.6	53.5	11.1
J5 (deg)	9.2	10.1	3.4	3.3
J6 (deg)	54.9	37.9	52.6	9.6

B. *Calibration with Different Robot Configurations and Noisy Data*

The industrial robotic manipulator IRB1600 was created in simulation using its DH parameters [9]. The laser pointer was fixed on the end-effector toward the X-axis in the end-effector frame, with the accurate parameters of $(\mathrm{M}_E = 1, N_E = 0, P_E = 0)$ and $(x_{0E} = 0, y_{0E} = 0, z_{0E} = 0)$. The center of PSD was located at the position (800mm, 100mm, 600mm) w.r.t robot base frame (it is unknown for the solution). A virtual PSD was built as a feedback to locate the laser beam on the center of the PSD surface. A real robot joint has limited resolution and robot localization noise even though the precise PSD-based feedback system is used. Therefore, we add noise to the joint and the position of the PSD in order to make the simulation more realistic. Combing the encoder resolution and position sensor noise ($\pm 2\mu$m), we can safely assume the maximum noise of robot localization is $\pm 0.05mm$ (equal to the repeated accuracy). Let PSD locate at different positions and laser aiming at the PSD center with eight positions and orientations rotating about x-axis and y-axis in the base frame, respectively. Coordinates of PSD center are P1 ($900mm, -50mm, 400mm$) w.r.t robot base frame (it is unknown for the solution).

Table II shows the results of the calibration with the PSD position of P1. Column 2 shows the actual offset parameters used by the simulation. Column 3 shows the mean error of the parameters identified by repeating the experiment five times with random localization error within $\pm 0.05mm$. Column 4 shows the standard deviation of the parameters errors with respect to the actual values. Column 5 and Column 6 show the mean and standard deviation of the parameters errors by repeating the experiment with pattern I configuration. From column 3 and column 4 mean error and standard deviation error of joint 2 are –1.2 degree and 0.56 degree, which is far away from the actual value of –0.4 degree. Results show offset parameter of joint 2 can not be identified and consequently the offset parameter of joint 3 is affected with pattern II. From column 5 and column 6 mean error and standard deviation error of all parameters are small (10^{-2}) with the big localization noise of $\pm 0.05mm$. It verify the calibration method is feasible with the optimum pattern I

configuration. Results justify robot configuration plays a big effect on the calibration solution. The experimental result is consistent with the mathematical analysis in section III-F.

TABLE II
SIMULATION RESULTS WITH NOISY DATA AT P1

Parameters	Actual Value	pattern II configuration		pattern I configuration	
		Mean Error ($\times 10^{-2}$)	STD ($\times 10^{-2}$)	Mean Error ($\times 10^{-2}$)	STD ($\times 10^{-2}$)
δ_2 (deg)	-0.4	-118.93	56.36	-1.69	0.02
δ_3 (deg)	0.5	2.11	16.23	1.98	1.02
δ_4 (deg)	-0.7	-3.20	3.38	-9.40	2.61
δ_5 (deg)	-0.5	0.07	0.08	-6.89	1.23
M_E	1.0	0.00	0.00	0.00	0.00
N_E	0.0	0.076	0.054	-0.084	0.02
y_{0E} (mm)	0.0	-0.048	0.093	-0.061	0.082
z_{0E} (mm)	0.0	-0.0835	0.0502	-0.253	0.137

C. Calibration Experiment of IRB1600 Robot

The calibration experiment was implemented on the ABB manipulator IRB1600. Based on the oberservation of the simulation, pattern I configuration and mixed pattern I and pattern II (four poses from pattern I and other four poses from pattern II) were chosen. The experiments are repeated mutiple times.

TABLE III
OFFSET CALIBRATION RESULTS OF IRB1600 ROBOT

Parameters	Initial Values	Mean	STD($\times 10^{-2}$)
δ_2 (deg)	0.0	0.8420	7.61
δ_3 (deg)	0.0	-0.8749	3.34
δ_4 (deg)	0.0	0.2881	1.34
δ_5 (deg)	0.0	0.1843	0.13
M_E	1.0	0.9999	0.00
N_E	0.0	-0.0012	0.62
y_{0E} (mm)	0.0	-0.282	0.57
z_{0E} (mm)	0.0	-0.652	0.61

Table III shows the results of the offset calibration experiment implemented on the ABB manipulator IRB1600. Column 3 shows the mean of parameters, and column 4 shows the standard deviation of the parameters from repeated experiments. The standard deviation of the parameters was small (10^{-2}), indicating the stability of the calibration method.

V. CONCLUSIONS

Robot joint offset has a much larger influence on robot positioning accuracy after leaving the robot factory for the end user. Using our proposed virtual lines-based single-point constraint approach, a portable, low-cost, battery-powered, wireless and automated calibration system was implemented. The mapping of the PPD was performed, and the error was analyzed. The errors in joint space are magnified in PSD plane, and consequently the resolution in the joint space is improved. The sensitivities of the calibration system were formulated mathematically, and verified pattern I was more efficient. Two types of patterns were experimented, and experimental results show pattern I configuration was a better configuration for the calibration issue. Both simulation and experimental results verified the feasibility of the sensitivity analysis and demonstrated the method can identify joint offset with un-calibrated laser tool parameters.

ACKNOWLEDGMENT

The authors would also like to thank Dr. George Zhang, Dr. Heping Chen, Dr. Thomas A. Fuhlbrigge, and Ms. Xiongzi Li of ABB for their technical advice and help during the process of this research.

REFERENCES

[1] M. R. Driels, L. W. Swayze, and L. S. Potter, "Full-pose calibration of a robot manipulator using a coordinate measuring machine," *Int. J. Adv.Manuf. Techno.*, vol. 8, no. l, pp. 34–41, 1993.

[2] M. Vincze, J. P. Prenninger, and H. Gander, "A laser tracking system to measure position and orientation of robot end effectors under motion," *Int. J. Robot. Res.*, vol. 13, pp. 305–314, 1994.

[3] M. A. Meggiolaro, G. Scriffignano, and S. Dubowsky, "Manipulator calibration using a single endpoint contact constraint," presented at the 26th Biennial Mech. Robot. Conf. 2000 ASME Design Eng. Tech. Conf., Baltimore, MD, Sep. 2000.

[4] H. Zhuang, S. H. Motaghedi, and Z. S. Roth, "Robot calibration with planar constraints," in *Proc. IEEE Int. Conf. Robot. Autom.*, Detroit, MI, 1999, pp. 805–810.

[5] M. Ikits and J. M. Hollerbach, "Kinematic calibration using a plane constraint," in *Proc. IEEE Int. Conf. Robot. Autom.*, 1997, pp. 3191–3196.

[6] W. S. Newman and D.W.Osborn, "A new method for kinematic parameter calibration via laser line," in *Proc. IEEE Int. Conf. Robot. Autom.*, 1993, vol. 2, pp. 160–165.

[7] H. Chen, T. Fuhlbrigge, S. Choi, et al. "Practical Industrial Robot Zero Offset Calibration," IEEE Conference on Automation Science and Engineering, 23-26 Aug. 2008.

[8] C. S. Gatla, R. Lumia, J. Wood, and G. Starr, "Calibration of industrial robots by magnifying errors on a distant plane," presented at the IEEE Int. Conf. Intell. Robots Syst., San Diego, CA, Oct. 29–2 Nov. 2007.

[9] Y. Liu, N. Xi, G. Zhang, X. Li, H. Chen, C. Zhang, M.J. Jeffery and T.A. Fuhlbrigge. "An Automated Method to Calibrate Industrial Robot Joint Offset Using Virtual Line-based Single-point Constraint Approach." Accepted to the IEEE Conference on Intelligent and Robots and Systems, 2009.

[10] J. Denavit, R.S. Hartenberg. "A Kinematic Notation for Lower Pair Mechanisms Based on Matrices, " J. Appl. Mech. ASME, June 1955, pp. 215-221.

[11] Y. Liu, N. Xi, Y. Shen, et al. "High-Accuracy Visual/PSD Hybrid Servoing of Robotic Manipulator," IEEE /ASME international conference on AIM, 2-5 July 2008.

[12] Kenneth Levenberg. "A Method for the Solution of Certain Non-Linear Problems in Least Squares". *The Quarterly of Applied Mathematics* **2**: 164 – 168. 1944.